

Towards a wave–extraction method for numerical relativity: III. Analytical examples for the Beetle–Burko radiation scalar

Lior M. Burko^{1,2}, Thomas W. Baumgarte^{3,4}, and Christopher Beetle^{5,6}

¹ *Department of Physics and Astronomy, Bates College, Lewiston, Maine 04240*

² *Department of Physics, University of Alabama in Huntsville, Huntsville, Alabama 35899*

³ *Department of Physics and Astronomy, Bowdoin College, Brunswick, Maine 04011*

⁴ *Department of Physics, University of Illinois at Urbana–Champaign, Urbana, Illinois 61801*

⁵ *Department of Physics, Florida Atlantic University, Boca Raton, Florida 33431*

⁶ *Perimeter Institute for Theoretical Physics, Waterloo, Ontario N2L 2Y5, Canada*

(Dated: draft of November 24, 2018)

Beetle and Burko recently introduced a background–independent scalar curvature invariant for general relativity that carries information about the gravitational radiation in generic spacetimes, in cases where such radiation is incontrovertibly defined. In this paper we adopt a formalism that only uses spatial data as they are used in numerical relativity and compute the Beetle–Burko radiation scalar for a number of analytical examples, specifically linearized Einstein–Rosen cylindrical waves, linearized quadrupole waves, the Kerr spacetime, Bowen–York initial data, and the Kasner spacetime. These examples illustrate how the Beetle–Burko radiation scalar can be used to examine the gravitational wave content of numerically generated spacetimes, and how it may provide a useful diagnostic for initial data sets.

PACS numbers: 04.25.Dm, 04.30.Nk, 04.70.Bw

I. INTRODUCTION

Compact binary systems of co-orbiting neutron stars or black holes are among the most promising sources of gravitational waves for a set of recently-constructed interferometric detectors, including the Laser Interferometer Gravitational Wave Observatory (LIGO). A substantial effort has been underway for some years now to model these systems theoretically, and thereby establish detailed predictions for comparison with experimental data. These predictions will likely be needed not only for verification of the theory, but for constructing filters needed to separate signal from noise in the detectors. Because a compact binary system admits no obvious symmetry or approximation, the theoretical problem is being tackled primarily within the field of numerical relativity, which aims to integrate directly the full Einstein field equations on the computer.

A numerical solution of the Einstein equations usually proceeds in three steps (see, e.g., [1] for a recent review and references). The first step solves the constraint equations of general relativity to find initial data for the problem. The second then evolves these data forward in time using the remaining field equations. In the third step the numerical solution of the second step is interpreted physically. This paper—as the other papers in this series—is interested in the third, last step of numerical relativity. Although conceptually straightforward, this program encounters many technical difficulties which make it seem unlikely that numerical relativity will be able to evolve compact binaries for many orbits (see, e.g., [2, 3, 4] and [5] for recent progress). Within the field, the consensus answer to these difficulties is to start the simulations using initial data which describe the system at small binary separations, shortly before coalescence. This approach introduces a fresh conceptual problem, however. It is far from clear how to pick initial data at small separation so as to replicate the outgoing wave pattern which would arise during a gradual inspiral from large separation. Intuitively, generic data describing a close binary will contain spurious radiation originating in the particular mathematical technique used to solve the constraint equations rather than in the astrophysics of the problem. In fact, it is known that different methods of solving the constraint equations lead to physically distinct initial data (see, e.g., [1, 6, 7]).

This paper is the third in a series which outlines a scheme to analyze the radiation content of a given spacetime using invariant techniques based solely on the physical metric. More specifically, this paper uses an invariant *radiation scalar* to measure the amount of radiation, including spurious radiation, in a variety of initial data sets familiar to the numerical relativity community. In general, a radiation scalar is a scalar function on spacetime derived from the physical metric which, when spacetime unambiguously describes gravitational radiation propagating in some background, manifestly contains information only about the radiative degrees of freedom. There may be many such metric invariants which could be defined. We will focus on just one, denoted ξ , which we call the BB radiation scalar [8]. This particular scalar seems well-suited to problems, like binary black-hole inspiral, where the quiescent end-state describes weak radiation propagating outside a single black hole approaching equilibrium. Ultimately, the idea would be to minimize in some sense this measure of radiation content and thereby identify more physically reasonable binary initial data sets. While this intuitive idea is easy to state, there are a number of caveats to taking

the picture it suggests too seriously. Nonetheless, the results of this paper suggest the radiation scalar approach could be used effectively in this way.

The definition of the BB scalar, and the scheme on which it is based, has certain strengths and limitations. In this context, the key strength of this approach lies in its direct applicability to initial data sets. (In addition, the BB scalar may also have intriguing applications for evolution data.) The only currently-known unambiguous way to minimize the spurious radiation content of such data is to use the evolution equations themselves. As evolution proceeds, spurious radiation will naturally propagate outward, and eventually off the numerical domain for the problem. The gravitational radiation remaining in the instantaneous data at later times would then be the astrophysically sound radiation generated by the binary at earlier times. However, the dynamical evolution also introduces numerical error, and the difficulties associated with this dynamical evolution, especially for binary black hole systems, motivated the construction of small-separation initial data in the first place. In contrast, the BB scalar may be calculated directly from an initial data set (see the first paper in this series [9], hereafter Paper I). No evolution is required. The approach also offers a potentially useful tool for the extraction of gravitational radiation from numerically evolved spacetimes (see [10], hereafter Paper II). However, here we focus exclusively on the application to initial data sets.

The main risk of the BB scalar approach lies in trying to push its physical interpretation beyond its appropriate scope. This point has been emphasized in previous papers [8, 9, 10] in this series. While mainly conceptual in origin, this issue raises genuine practical problems in applications like those considered in this paper.

The interpretation of the BB scalar is unambiguous when spacetime describes weak-wave perturbations of a single black hole, an approximation which becomes increasingly accurate at late times after coalescence of a binary system. In particular, it is certain to be small in this perturbative context. However, it remains calculable much more generally, although this precise physical interpretation is lost. This is hardly surprising since even the notion of gravitational radiation cannot be defined unambiguously in general regions of spacetime. More pragmatically, there is nothing to guarantee that the radiation scalar cannot be small in this broader context, where spacetime might intuitively be said to describe strong radiation fields. That is, although the radiation scalar is definitely small when little radiation is present, it may also be small coincidentally even when this is not the case. This can happen because, whereas ingoing and outgoing gravitational radiation in perturbation theory is intuitively associated with the two Newman–Penrose Weyl curvature components ψ_0 and ψ_4 measured in a particular null-tetrad frame, the BB scalar measures just their product: $\xi = \psi_0 \psi_4$. Thus, in an extreme example, even though the outgoing component of the radiation field described by ψ_4 may be non-perturbatively large, if the ingoing component ψ_0 vanishes then so does ξ . However, this cannot happen accidentally. Intuitively, outgoing radiation will scatter off the fixed potential described by the background in which it propagates to produce an ingoing signal. The outgoing signal would have to be very carefully tuned to the background in order to have the net effects of this back-scattering cancel exactly throughout some region of spacetime. The mathematical expression of this fact lies in the Teukolsky–Starobinsky identities, which interrelate the derivatives of the two seemingly independent components of the radiation field ψ_0 and ψ_4 in a Kerr black-hole background. Following this extreme example, one might reasonably expect situations wherein the BB scalar is coincidentally small are rare and non-generic. This paper tests that expectation using exact, analytical initial data sets whose gravitational wave content is already—independently—rather well understood. The results are encouraging. We find that, at least in these specific cases, the expectation that the radiation scalar should not be small coincidentally in typical situations of practical interest is indeed supported by the facts.

This paper is organized as follows. In Section II, we summarize the recipe developed in Paper I for extracting the BB scalar from 3+1 Cauchy data for the gravitational field. The following three sections explicitly calculate the BB scalar in three different continuous families of analytical initial data sets. Section III focuses on linearized wave propagating on a flat background. This is a worthwhile test because the BB scalar was explicitly developed as a tool to analyze such linearized waves propagating around a Kerr black hole. In fact, the presence of a dominant background component, associated with the “Coulombic” Kerr geometry, has been used explicitly to define the BB scalar. It is therefore noteworthy that the approach is also effective when such a dominant Coulombic field is absent. Section IV turns to genuine black hole solutions, analyzing Bowen–York initial data for single black holes using the BB scalar. This is probably the most physically significant application considered here. It finds that, whereas the BB scalar does vanish in the Kerr spacetime where clearly no radiation is present, it does not vanish for the Bowen–York data. We explicitly find a quartic growth of ξ with the angular momentum L of the Bowen–York hole. This is exactly what one would naively have expected. Section V calculates the BB scalar in the cosmological Kasner solution. We do this to illustrate both the limitations and the ancillary benefits of our approach. The BB scalar does *not* vanish in these spacetimes, even though they are understood to contain no radiation. However, this is not surprising since these cosmological solutions do not contain a radiation zone in which the usual physical meaning could be attached to the BB scalar. Nonetheless, we find that it *can* be used as an interesting gauge-invariant tool to partially characterize the gravitational field in this context. One must only resist the temptation to think of it as a *radiation* scalar. Finally, Section VI summarizes our results and makes a few further comments regarding their interpretation.

II. RECIPE

This Section closely follows the method of paper I to construct the BB scalar ξ from numerical relativity data. We refer to paper I [9] for further details and discussion of this recipe. It is recapitulated here only for convenience.

We begin our discussion at the level of spacetime geometry, where the Weyl curvature tensor picks out exactly three null tetrads, up to certain scaling transformations, at a generic event¹. These are the “transverse frames” in which the Newman–Penrose curvature components ψ_1 and ψ_3 vanish. At sufficiently large distances from the sources, in a radiation zone, it is possible to single out one of these three, called the quasi-Kinnersley frame, on which our definitions are based. The name derives from a particular null tetrad introduced by Kinnersley on a particular spacetime, the stationary Kerr black hole, and subsequently used by Teukolsky to analyze the gravitational radiation content of perturbed black hole spacetimes. Teukolsky found that, when one makes perturbative corrections to the background Kinnersley tetrad to maintain vanishing Newman–Penrose curvature components ψ_1 and ψ_3 in the perturbed spacetime, the gravitational radiation is entirely encoded in the two curvature components ψ_0 and ψ_4 (see also [11]). The remaining non-zero component, ψ_2 , is intuitively associated with a Coulombic part of the field, and is dominated by terms deriving from the stationary background.

Once the quasi-Kinnersley frame has been identified in a radiation zone, its definition may then be carried into more general regions of spacetime using a continuity principle. The quasi-Kinnersley frame is always one of the three transverse frames at *any* point of spacetime, whether that point lies in a radiation zone or not. In these transverse frames, the Newman–Penrose scalar ψ_2 will typically take three distinct values, only one of which will lead to a *continuous* function when compared with *known* quasi-Kinnersley values of ψ_2 at nearby points. The frame so chosen is the quasi-Kinnersley frame. Put another way, the key idea is that there is no ambiguity in identifying the quasi-Kinnersley frame in a radiation zone, and maintaining continuity everywhere in spacetime generally determines a unique “transverse frame field” throughout. This is the quasi-Kinnersley frame, defined globally. The results of this paper will indicate that there ought to be little doubt in practice concerning which value of ψ_2 will give the desired continuous extension. See the Discussion for further comments.

This paper will consider two curvature scalars defined using the quasi-Kinnersley frame:

$$\chi := \psi_2 \quad \text{and} \quad \xi := \psi_0 \psi_4. \quad (1)$$

Each of these functions is understood to be defined on spacetime by evaluating the indicated Newman–Penrose curvature components *in the quasi-Kinnersley frame*. The first of these quantities, χ , is called the Coulomb scalar. The nomenclature derives from intuition in the Teukolsky formalism: ψ_2 is dominated by the stationary, Coulombic field of the background Kerr black hole. The second quantity, ξ , is the BB radiation scalar. In a radiation zone accurately described by the Teukolsky formalism, it manifestly depends only on the radiative degrees of freedom. Although the components ψ_0 and ψ_4 are not separately preserved by the residual scaling transformations of the null tetrad allowed by the Weyl curvature, their product is. Thus, the BB scalar is a true invariant derived from spacetime curvature.

Although certainly not a radiation scalar, the Coulomb scalar is still quite useful in our approach. First, as described above, demanding continuity of χ plays the key role in defining the quasi-Kinnersley frame. We could also have used continuity of ξ to do this, but ξ is quadratic in the curvature while whereas χ is only linear. The radiation scalar therefore falls off much more rapidly ($\xi \sim r^{-6}$) at large distance than the Coulomb scalar ($\chi \sim r^{-3}$), making the numerical problem of determining continuity much harder. Second, the Coulomb scalar can be used to extract information about the single black hole underlying a perturbation-theoretic description of a given spacetime. Thus, for example, it may be used at late times to determine, or at least constrain estimates of, the mass and spin of the final black hole resulting from coalescence in a background-independent way.

Numerical relativity is not primarily concerned with spacetime geometry. Rather, it solves a Cauchy problem for general relativity, calculating a series of spatial geometries parameterized by a fiducial time variable. These may then be assembled to form spacetime. The assembly procedure can of course be done analytically, and used to express the BB scalar in terms of given Cauchy data. This has been done in Paper I, and we describe the results here.

In a 3 + 1 decomposition, the gravitational fields are expressed in terms of a spatial metric γ_{ij} and an extrinsic curvature K_{ij} . The electric and magnetic components E_{ij} and B_{ij} of the spacetime Weyl tensor can be computed

¹ Where spacetime is of algebraic Petrov types I or D, there are three such frames. Where spacetime is type II, there is only one. In the remaining cases, types III and N, no such frames exist. These last cases, though, are far from generic, and ought not arise in the situations of interest here. By far, the most probable algebraic type at a typical point of the spacetimes we study is type I.

from these data using

$$\mathcal{E}_{ij} = R_{ij} + KK_{ij} - K_{ik}K_j{}^k - 4\pi S_{ij} \quad (2)$$

$$E_{ij} = \mathcal{E}_{ij} - \frac{1}{3}\gamma_{ij}\gamma^{kl}\mathcal{E}_{kl} \quad (3)$$

where $S_{ij} = \gamma_i{}^a\gamma_j{}^b T_{ab}$ is the spatial projection of the stress energy tensor T_{ab} , and R_{ij} is the spatial Ricci tensor (see, e.g., Ref. [1] for more detail). The definition for the magnetic part of the spacetime Weyl tensor depends on the convention used for the extrinsic curvature and for the spacetime volume element. We adopt here the convention that

$$K_{ij} = -\frac{1}{2}\mathcal{L}_n \gamma_{ij}, \quad (4)$$

where \mathcal{L}_n denotes the Lie derivative in the direction of the normal n^a to the 3-hypersurface. Our convention for the spacetime volume element is

$$\epsilon_{abcd} = 24 i \ell_{[a} n_b m_c \bar{m}_{d]} \quad (5)$$

(see paper I for more detail.) We next define the magnetic part of the spacetime Weyl tensor

$$\mathcal{B}_{ij} = -\epsilon_i{}^{kl}\nabla_k K_{lj} \quad (6)$$

$$B_{ij} = \mathcal{B}_{(ij)}. \quad (7)$$

By construction, E_{ij} and B_{ij} are both symmetric and traceless. We then define the complex tensor²

$$C^i{}_j = E^i{}_j + i B^i{}_j, \quad (8)$$

from which the scalar curvature invariants I and J can be computed as

$$I = \frac{1}{2}C^i{}_j C^j{}_i \quad (9)$$

and

$$J = -\frac{1}{6}C^i{}_j C^j{}_l C^l{}_i. \quad (10)$$

Once a basis is chosen, the tensor $C^i{}_j$ becomes simply a 3×3 matrix. In ordinary linear algebra, it is well-known that any scalar invariant which may be extracted from such a matrix must be expressible as a function of three basic invariants. These basic invariants may be chosen to be the eigenvalues or, for example, the traces of the first three powers of the matrix in question. The trace of our matrix vanishes because it derives from the spacetime Weyl tensor, and the traces of its square and cube are basically I and J . Thus, we should expect our Coulomb and BB scalars may be expressed as functions of I and J . To do this, we recall the Baker–Campanelli speciality index [13] defined by

$$S := 27 \frac{J^2}{I^3}. \quad (11)$$

In terms of S , the Coulomb scalar can be written as

$$\chi^{0,\pm} = -\frac{3J}{2I} \frac{W_\chi(S)^{1/3} + W_\chi(S)^{-1/3}}{\sqrt{S}}, \quad (12)$$

² Note that the relative sign in the definition of $C^i{}_j$ here differs from that used in Paper I. At first glance, it would appear that the quantities we calculate here are therefore the complex conjugates of those calculated there. The difference, however, is illusory. Our previous papers have tacitly assumed a definition for the extrinsic curvature with the opposite sign to that in Eq. (4). While the previous convention is popular in the mathematical relativity community (see, e.g., [12]), the current one is used more often in the numerical relativity community. We therefore adopt it here for the convenience of the latter. As a result of this shift of convention, the sign of the tensor \mathcal{B}_{ij} defined above is reversed. We compensate this reversal in the definition of $C^i{}_j$ so that this tensor takes the exact same value on a Cauchy slice with our new conventions as it did with the old. With this one modification, all other formulae from the previous papers continue to hold unmodified.

where $W_\chi(S) = \sqrt{S} - \sqrt{S-1}$, while the BB scalar is

$$\xi^{0,\pm} = \frac{1}{4} I \left[2 - W_\xi(S)^{1/3} - W_\xi(S)^{-1/3} \right], \quad (13)$$

where $W_\xi(S) = 2S - 1 + 2\sqrt{S(S-1)}$. In general, both the Coulomb and BB scalars admit three distinct complex roots, associated with the three distinct transverse frames. We denote these three roots with the superscripts “0, \pm ”. The value in the principal branch of the root functions above has superscript 0, and this branch defines the quasi-Kinnersley frame in an appropriate radiation zone. The other two branches have superscripts \pm . Either of these may be labeled the quasi-Kinnersley value in the interior of spacetime, depending on what is needed to maintain continuity while coming in from the radiation zone. We will illustrate this point explicitly below.

In addition to the direct calculation above, there are two other ways to compute $\xi^{0,\pm}$ and $\chi^{0,\pm}$. The first is to solve the eigenvalue problem for the complex spatial tensor C^i_j :

$$C^i_j \hat{\sigma}^j = \lambda \hat{\sigma}^i = (2\chi^{0,\pm}) \hat{\sigma}^i. \quad (14)$$

As shown in Paper I, the three eigenvalues λ turn out to be exactly twice the Weyl scalar ψ_2 evaluated in the three transverse frames. Thus, the Coulomb scalar at any point of spacetime is always half of one of the eigenvalues of C^i_j . If these eigenvalues are calculated, this approach does not say which is which, so it is not immediately clear which eigenvalue is associated with the principal branch of (12), and therefore with the quasi-Kinnersley frame. However, it has been shown in Paper II that, among the three branches, the principal value has the largest modulus in a radiation zone. Thus, the prescription to calculate the Coulomb scalar is to take half the eigenvalue of largest modulus at large distances, and extend inward to strong-field regions always choosing the unique eigenvalue which keeps the function χ smooth. In a transverse frame, the Newman–Penrose Weyl scalars ψ_1 and ψ_3 vanish by definition, and this gives a particularly simple relation between the Coulomb and BB scalars:

$$\xi^{0,\pm} = (\psi_0 \psi_4)^{0,\pm} = I - 3 \left(\psi_2^{0,\pm} \right)^2. \quad (15)$$

Thus, if the Coulomb scalar is known, the radiation scalar follows immediately. The second way to calculate the Coulomb and BB scalars is to use series expansions of the exact formulae above. As shown in paper I, for a spacetime that asymptotically is perturbed about algebraic speciality, we can expand

$$\chi = -3 \frac{J}{I} \left[1 - \frac{4}{9} (S-1) + \frac{80}{243} (S-1)^2 + \dots \right], \quad (16)$$

and

$$\xi = -\frac{I}{9} (S-1) \left[1 - \frac{8}{27} (S-1) + \frac{112}{729} (S-1)^2 \dots \right]. \quad (17)$$

These expansions explicitly use the principal values of the root functions in (12) and (13), and therefore allow us to identify the quasi-Kinnersley χ and ξ asymptotically. This technique can be useful numerically when all three values $\chi^{0,\pm}$ become small. We illustrate this fact in Sections IV B for Bowen–York data and V for the Kasner spacetime.

III. LINEARIZED WAVES ON A FLAT BACKGROUND

Probably the first example that comes to mind when evaluating a radiation scalar are pure wave solutions. Unfortunately, the simplest such solution, plane waves, is too simple to be of interest. Plane waves are Petrov type N, and hence algebraically special. In a type N spacetime, a frame can always be found so that ψ_4 is the only non-vanishing Weyl scalar. This frame is automatically transverse, so that $\xi = \psi_0 \psi_4$ vanishes identically. As the BB scalar is frame-independent, it vanishes also in all other, non-canonical frames. In a plane wave spacetime the BB scalar vanishes despite the presence of gravitational radiation.

We therefore turn to two less trivial examples, namely linearized time-symmetric Einstein–Rosen cylindrical gravitational waves in Section III A and linearized even-parity quadrupole Teukolsky waves in Section III B.

A. Linearized Einstein–Rosen cylindrical waves

The metric for Einstein–Rosen cylindrical waves of amplitude B and pulse width a [14] is given by

$$ds^2 = e^{2[\gamma(t,\rho) - \psi(t,\rho)]} (-dt^2 + d\rho^2) + e^{2\psi(t,\rho)} dz^2 + \rho^2 e^{-2\psi(t,\rho)} d\phi^2, \quad (18)$$

where

$$\psi(t, \rho) = B \left[\frac{1}{\sqrt{(a+it)^2 + \rho^2}} + \frac{1}{\sqrt{(a-it)^2 + \rho^2}} \right] \quad (19)$$

(which is a real function.) In what follows we consider linearized waves, so that we can take the function $\gamma(t, \rho)$, which is quadratic in B , to vanish. The solution is time-symmetric about $t = 0$, and describes cylindrical waves that are imploding on the symmetry axis for $t < 0$ and exploding for $t > 0$.

In the context of numerical relativity, the spacetime metric is usually expressed in terms of a lapse α , a shift β^i and a spatial metric γ_{ij} . These quantities can be found by identifying the spacetime metric (18) with the ‘‘ADM’’ form

$$ds^2 = -\alpha^2 dt^2 + \gamma_{ij}(dx^i + \beta^i dt)(dx^j + \beta^j dt), \quad (20)$$

Here the shift vanishes identically, $\beta^i = 0$, the lapse is

$$\alpha = \exp[-\psi(t, \rho)], \quad (21)$$

and the spatial metric is

$$d\sigma^2 = e^{2[-\psi(t, \rho)]} d\rho^2 + e^{2\psi(t, \rho)} dz^2 + \rho^2 e^{-2\psi(t, \rho)} d\phi^2. \quad (22)$$

We also compute the extrinsic curvature K_{ij} from Eq. (4)

$$K_{ij} = -\frac{1}{2\alpha} (\partial_t \gamma_{ij} - D_i \beta_j - D_j \beta_i), \quad (23)$$

where D_i is the covariant derivative compatible with the spatial metric γ_{ij} , and where we use the sign convention typically used in numerical relativity.

At the moment of time symmetry $t = 0$, K_{ij} vanishes identically, which greatly simplifies the problem. The only non-vanishing term in the electric (3) or magnetic (7) components of the Weyl tensor is then the Ricci tensor R_{ij} in the electric part E_{ij} , which yields

$$\begin{aligned} E_\rho^\rho &= -2B (\rho^2 + a^2)^{-3/2} \\ E_z^z &= 2B (2a^2 - \rho^2) (\rho^2 + a^2)^{-5/2} \\ E_\phi^\phi &= 2B (2\rho^2 - a^2) (\rho^2 + a^2)^{-5/2} \end{aligned} \quad (24)$$

to linear order in B (all other components vanish.) At $t = 0$ we therefore have $C^i_j = E^i_j$. Using (9) and (10) we find the curvature invariants

$$I = 12B^2 \frac{a^4 - a^2\rho^2 + \rho^4}{(\rho^2 + a^2)^5} \quad (25)$$

and

$$J = -4B^3 \frac{(2\rho^2 - a^2)(\rho^2 - 2a^2)}{(\rho^2 + a^2)^{13/2}}, \quad (26)$$

and from (11) the speciality index

$$S = \frac{(2\rho^2 - a^2)^2 (\rho^2 - 2a^2)^2 (\rho^2 + a^2)^2}{4(a^4 - a^2\rho^2 + \rho^4)^3}. \quad (27)$$

We plot the speciality index S as a function of ρ in the upper panel of Fig. 1. Interestingly, S is independent of the wave amplitude B and therefore does not provide a measure of the strength of the gravitational radiation.

Since S is independent of B , the Coulomb scalar χ (12) must scale with B and the BB scalar ξ (13) with B^2 . Reversing this argument we can see that the speciality index S must be independent of the wave amplitude whenever the Coulomb scalar is perturbative and scales with B , while the BB scalar scales with B^2 . We find the same behavior for the Teukolsky waves in Section III B.

For the remainder of this Section we determine the Coulomb scalar χ and the BB radiation scalar ξ explicitly as functions of ρ , adopting the following strategy. There are three regions for which the spacetime is close to speciality,

i.e., for which $S - 1 \ll 1$: $\rho \gg a$, $\rho = a$ and $\rho \ll a$ (compare Fig. 1.) We then identify χ with an eigenvalue of C_j^i . Specifically, we require that at asymptotically great distances ($\rho \gg a$) the expansion (16) holds, and then identify χ with an eigenvalue of C_j^i — which is equivalent to picking a particular branch in the cubic roots in (12). From χ we can then compute ξ using (15). Finally, we require continuity and differentiability as we move to smaller and smaller values of ρ/a .

Before we proceed we list the three eigenvalues of C_j^i , which we denote λ_ρ , λ_z and λ_ϕ ,

$$\begin{aligned}\lambda_\rho &= -2B (\rho^2 + a^2)^{-3/2} \\ \lambda_z &= 2B (2a^2 - \rho^2) (\rho^2 + a^2)^{-5/2} \\ \lambda_\phi &= 2B (2\rho^2 - a^2) (\rho^2 + a^2)^{-5/2}.\end{aligned}\tag{28}$$

Notice that $I = (1/2) \sum_i \lambda_i^2$ and $J = (1/2) \Pi_i \lambda_i$ as expected.

To find χ and ξ we examine the asymptotic region $\rho \gg a$. In this limit,

$$I \approx \frac{12}{\rho^6} B^2 \quad \rho \gg a,\tag{29}$$

and

$$J \approx -\frac{8}{\rho^9} B^3 \quad \rho \gg a,\tag{30}$$

so that (16) yields

$$\chi \approx -3 \frac{J}{I} \approx \frac{2}{\rho^3} B. \quad \rho \gg a,\tag{31}$$

This the quasi-Kinnersley χ . We compare this result with the limiting values of the three eigenvalues (28) of the tensor C_j^i ,

$$\lambda_\rho \approx -\frac{2}{\rho^3} B, \quad \lambda_z \approx -\frac{2}{\rho^3} B, \quad \lambda_\phi \approx \frac{4}{\rho^3} B \quad \rho \gg a,\tag{32}$$

The eigenvalue that corresponds to χ is the one that satisfies $\lambda = 2\chi$, and therefore we conclude that for $\rho \gg a$, the correct eigenvalue is λ_ϕ . (Alternatively, this is the eigenvalue with the greatest modulus — see paper II.) Next, we require that χ is smooth to extend χ to other regions of the spacetime. In principle, we could switch to a different eigenvalue at a branch point. This would make χ discontinuous, however, which is not desirable. A distributional χ would suggest similar characteristics of the physical Weyl scalar, which is clearly not the case in this example. The only identification for ξ that makes it smooth throughout is that $\chi = \lambda_\phi/2$ not just for $\rho \gg a$, but everywhere. We therefore have

$$\chi = \frac{2\rho^2 - a^2}{(\rho^2 + a^2)^{5/2}} B\tag{33}$$

everywhere. We can now compute the BB radiation scalar ξ from (15), which yields

$$\xi = I - 3\chi^2 = 9 \frac{a^4}{(\rho^2 + a^2)^5} B^2.\tag{34}$$

Our results for χ and ξ are plotted in Fig. 1 in the middle and lower panels, correspondingly.

In Appendix A we present an alternative, yet equivalent, derivation of χ and ξ , that is based directly on Eqs. (12) and (13), respectively.

B. Linearized quadrupole waves

Einstein–Rosen cylindrical waves are not asymptotically flat, which limits their usefulness as testbeds for numerical relativity. (In addition, Einstein–Rosen cylindrical waves do not represent the exterior solution of bounded radiating systems.) We therefore briefly discuss a second example of linearized gravitational waves over a flat background,

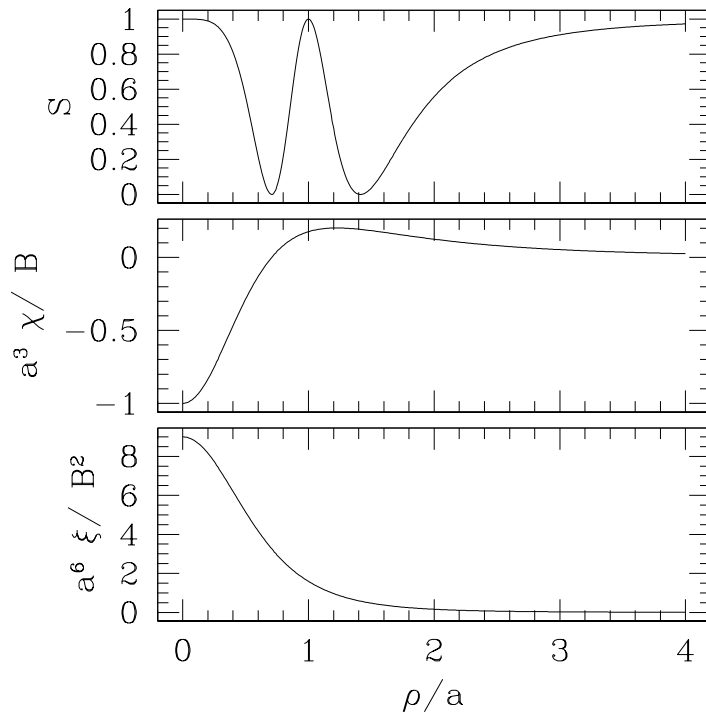


FIG. 1: The speciality index S (upper panel), the dimensionless Coulomb scalar $a^3 \chi/B$ (middle panel), and the dimensionless BB scalar $a^6 \xi/B^2$ (lower panel), as functions of ρ/a for time-symmetric linearized Einstein–Rosen cylindrical waves of pulse width a , at $t = 0$.

namely Teukolsky’s even-parity linearized quadrupole gravitational waves in vacuum with azimuthal symmetry [15]. This spacetime is algebraically-general (Petrov type I), that asymptotically at great distances ($\lambda^{1/2} r \gg 1$) approaches algebraic speciality (Petrov type III). This algebraic class will be important for the interpretation of the speciality index S and the BB scalar ξ .

From the spacetime metric (Eq. (5) in [15]) we find the lapse α to be unity, the shift β^i to vanish, and we can identify the spatial metric γ_{ij} as

$$d\sigma^2 = [1 + (2 - 3 \sin^2 \theta) \mathcal{A}] dr^2 - 6 \mathcal{B} r \sin^2 \theta \cos \theta dr d\theta + (1 - \mathcal{A} + 3 \sin^2 \theta \mathcal{C}) r^2 d\theta^2 + [1 + (3 \sin^2 \theta - 1) \mathcal{A} - 3 \sin^2 \theta \mathcal{C}] r^2 \sin^2 \theta d\phi^2. \quad (35)$$

Here the coefficients \mathcal{A} , \mathcal{B} and \mathcal{C} are given in terms of a function $F(x) := F(t \mp r)$ and its derivatives $F^{(n)} \equiv d^n F(x)/dx^n|_{x=t \mp r}$,

$$\mathcal{A}_{\mp} = 3 \left(\frac{F^{(2)}}{r^3} \pm \frac{3F^{(1)}}{r^4} + \frac{3F}{r^5} \right) \quad (36)$$

$$\mathcal{B}_{\mp} = - \left(\pm \frac{F^{(3)}}{r^2} + \frac{3F^{(2)}}{r^3} \pm \frac{6F^{(1)}}{r^4} + \frac{6F}{r^5} \right) \quad (37)$$

$$\mathcal{C}_{\mp} = \frac{1}{4} \left(\frac{F^{(4)}}{r} \pm \frac{2F^{(3)}}{r^2} + \frac{9F^{(2)}}{r^3} \pm \frac{21F^{(1)}}{r^4} + \frac{21F}{r^5} \right), \quad (38)$$

where the upper/lower signs correspond to that in the definition of F . We would like to construct time-symmetric data with $K_{ij} = 0$ at $t = 0$, and therefore choose linear combinations $\mathcal{A} = \mathcal{A}_- - \mathcal{A}_+$, $\mathcal{B} = \mathcal{B}_- - \mathcal{B}_+$, and $\mathcal{C} = \mathcal{C}_- - \mathcal{C}_+$. For concreteness, we choose the function

$$F(x) = \epsilon (t \pm r)^5 e^{-\lambda(t \pm r)^2} \quad (39)$$

where ϵ is a measure of the wave amplitude and λ is related to the wavelength.

As for Einstein–Rosen waves, the vanishing of the extrinsic curvature at $t = 0$ greatly simplifies the problem. Since the spatial Ricci tensor R_{ij} is linear in ϵ , we have $\mathcal{E}_{ij} = R_{ij}$ to leading order in ϵ and also $B_{ij} = 0$. This scaling is sufficient to determine the scaling of the BB radiation scalar ξ : Since $C^i_j = E^i_j$ is linear in ϵ , I must scale with ϵ^2 and J with ϵ^3 . We again find that the speciality index S is independent of ϵ . It does depend on the choice of $F(x)$, but is independent of the wave amplitude. That is, S is insensitive to the amplitude of the waves. As we demonstrate in Appendix B, the speciality index $S \rightarrow 0$ as $\lambda^{1/2} r \rightarrow \infty$. However, as spacetime is asymptotically neither Petrov types 0 nor N, while $I, J \rightarrow 0$, it is algebraically special and of Petrov type III. This property is not accounted for by the speciality index S , which does not approach unity as $\lambda^{1/2} r \rightarrow \infty$.

The Coulomb scalar χ again scales with the wave amplitude parameter ϵ , while the BB scalar ξ scales with its square, ϵ^2 .

Explicit expressions for the Coulomb and BB radiation scalar can be constructed with an analysis similar to that in Section III A for Einstein–Rosen waves. The calculations are significantly more involved, however, and do not necessarily provide new insight. Instead of going through these calculations we assure the reader that the results are qualitatively very similar to those for Einstein–Rosen waves, and refer to Appendix B for some details.

IV. ROTATING BLACK HOLES

A. Kerr black holes

The Kerr solution is of Petrov type D and hence algebraically special with

$$S = 1, \quad (40)$$

independently of the black hole angular momentum $L = aM$. From Eq. (17) it is evident that the BB radiation scalar vanishes, $\xi = 0$. This can also be seen by observing that $W_\xi = 1$ when $S = 1$. The three cubic roots of unity are $1, e^{2i\pi/3}$ and $e^{4i\pi/3}$, which, when inserted into $\xi^{0,\pm}$, yield zero and twice $3I/4$. These are the three roots found in paper II, and the BB radiation scalar corresponds to the vanishing value. Given that the Kerr spacetime is stationary and does not contain any gravitational radiation it is reassuring that the radiation scalar vanishes.

Even though we already know the result, it is useful to demonstrate that the recipe laid out in Section II would lead to the same conclusion. To do so we start with the spacetime metric of a Kerr black hole, which in Boyer–Lindquist coordinates can be written as

$$ds^2 = -\frac{\rho^2 \Delta}{\Sigma} dt^2 + \frac{\Sigma}{\rho^2} \sin^2 \theta \left(d\phi - \frac{2MaR}{\Sigma} dt \right)^2 + \frac{\rho^2}{\Delta} dR^2 + \rho^2 d\theta^2 \quad (41)$$

where we have used the abbreviations $\Delta = R^2 - 2MR + a^2$, $\rho^2 = R^2 + a^2 \cos^2 \theta$, and $\Sigma = (R^2 + a^2)(R^2 + a^2 \cos^2 \theta) + 2a^2 MR \sin^2 \theta$. As in Section III A we can identify the spatial metric of constant Boyer–Lindquist time slices as

$$\gamma_{ij} dx^i dx^j = \frac{\rho^2}{\Delta} dR^2 + \rho^2 d\theta^2 + \frac{\Sigma}{\rho^2} \sin^2 \theta d\phi^2, \quad (42)$$

the lapse as

$$\alpha = \sqrt{\frac{\rho^2 \Delta}{\Sigma}} \quad (43)$$

and the shift vector as

$$\beta_a = (0, 0, -2MaR\rho^{-2} \sin^2 \theta). \quad (44)$$

From (23) we then find the only non-vanishing components of the extrinsic curvature (up to symmetry) to be

$$K_{R\phi} = \frac{aM\{3R^2\rho^2 + a^2[\rho^2 - 2(R^2 + a^2) \cos^2 \theta]\} \sin^2 \theta}{\rho^3 \Delta^{1/2} \Sigma^{1/2}} \quad (45)$$

and

$$K_{\theta\phi} = -2 \frac{Ma^3 R \Delta^{1/2} \sin^3 \theta \cos \theta}{\rho^3 \Sigma^{1/2}}. \quad (46)$$

The electric part of the Weyl tensor now can be computed from (3)

$$E_{RR} = -\frac{MR(2\Sigma + 3a^2\Delta \sin^2\theta)(\rho^2 - 4a^2 \cos^2\theta)}{\Delta\rho^4\Sigma} \quad (47)$$

$$E_{R\theta} = 3\frac{a^2M(R^2 + a^2)(3\rho^2 - 4a^2 \cos^2\theta) \sin\theta \cos\theta}{\rho^4\Sigma} \quad (48)$$

$$E_{\theta\theta} = \frac{MR(\rho^2 - 4a^2 \cos^2\theta)(\Sigma + 3a^2\Delta \sin^2\theta)}{\rho^4\Sigma} \quad (49)$$

$$E_{\phi\phi} = \frac{MR\Sigma(\rho^2 - 4a^2 \cos^2\theta) \sin^2\theta}{\rho^8} \quad (50)$$

and the magnetic part from (7)

$$B_{RR} = -\frac{aM(3\rho^2 - 4a^2 \cos^2\theta)(2\Sigma + 3a^2\Delta \sin^2\theta)}{\Delta\rho^4\Sigma} \cos\theta \quad (51)$$

$$B_{R\theta} = -3\frac{aMR(R^2 + a^2)(\rho^2 - 4a^2 \cos^2\theta)}{\rho^4\Sigma} \sin\theta \quad (52)$$

$$B_{\theta\theta} = -\frac{aM(3\rho^2 - 4a^2 \cos^2\theta)(\Sigma + 3a^2\Delta \sin^2\theta)}{\rho^4\Sigma} \cos\theta \quad (53)$$

$$B_{\phi\phi} = \frac{aM\Sigma(3\rho^2 - 4a^2 \cos^2\theta)}{\rho^8} \sin^2\theta \cos\theta. \quad (54)$$

From E_{ij} and B_{ij} we construct C_{ij} as well as the invariants I and J , following Section II. As expected we find

$$S = 1, \quad (55)$$

which is by no means surprising but reassuring.

B. Bowen–York Initial Data

Initial Data describing rotating black holes can also be constructed by solving the constraint equations in the Bowen–York [16] formalism. This approach assumes that the spatial metric is conformally flat. For rotating Kerr black holes, slices of constant Boyer–Lindquist time are not conformally flat, nor are axisymmetric foliations that smoothly reduce to slices of constant Schwarzschild time in the Schwarzschild limit [17]. This suggests that Bowen–York initial data give rise to a spacetime that is distinct from the Kerr–Schild spacetime. This was demonstrated explicitly by Gleiser, Nicasio, Price and Pullin ([18], hereafter GNPP), who used a perturbative calculation to show that Bowen–York initial data evolve into a spacetime that can be interpreted as a Kerr black hole with gravitational radiation. GNPP found that the amplitude of the emitted gravitational radiation scales with the square of the black hole’s angular momentum L , and the power accordingly with L^4 . As an important test we verify in this Section that the BB scalar picks up this gravitational radiation and identifies the correct scaling.

In a conformal transverse-traceless decomposition of the vacuum constraint equations the Hamiltonian constraint reduces to

$$8\bar{\nabla}^2\psi - \psi\bar{R} - \frac{2}{3}\psi^5K^2 + \psi^{-7}\bar{A}_{ij}\bar{A}^{ij} = 0 \quad (56)$$

and the momentum constraint is

$$\bar{\nabla}_j\bar{A}^{ij} - \frac{2}{3}\psi^6\bar{\gamma}^{ij}\bar{\nabla}_jK = 0 \quad (57)$$

(see, e.g., [1, 6, 19] for recent reviews). The conformal factor ψ relates the physical spatial metric γ_{ij} to the conformally related metric $\bar{\gamma}_{ij}$ via

$$\gamma_{ij} = \psi^4\bar{\gamma}_{ij}, \quad (58)$$

where $\bar{\nabla}_i$ and \bar{R} are the covariant derivative and scalar curvature associated with $\bar{\gamma}_{ij}$, and the extrinsic curvature K_{ij} is decomposed into its trace K and a traceless part \bar{A}_{ij} as

$$K_{ij} = \psi^{-2}\bar{A}_{ij} + \frac{1}{3}\gamma_{ij}K. \quad (59)$$

Assuming conformal flatness ($\bar{\gamma}_{ij} = \eta_{ij}$, where η_{ij} is the flat spatial metric in any coordinate system) and maximal slicing results in $\bar{R} = 0$ and $K = 0$, so that equations (56) and (57) reduce to

$$\bar{\nabla}^2 \psi = -\frac{1}{8} \psi^{-7} \bar{A}_{ij} \bar{A}^{ij} \quad (60)$$

and

$$\bar{\nabla}_j \bar{A}^{ij} = 0. \quad (61)$$

Here $\bar{\nabla}_i$ is now the flat covariant derivative associated with η_{ij} (as we assumed $\bar{\gamma}_{ij} = \eta_{ij}$).

The momentum constraint (61) decouples from the Hamiltonian constraint (60) under these assumptions and can be solved analytically. For a spinning, unboosted black hole in polar coordinates (i.e. $\bar{\gamma}_{ij} = \text{diag}(1, r^2, r^2 \sin^2 \theta)$) the only non-vanishing component of \bar{A}_{ij} is

$$\bar{A}_{r\phi} = \frac{3 \sin^2 \theta}{r^2} L \quad (62)$$

where L is the angular momentum [16].

Given the angular momentum L and Eq. (62), the conformal factor ψ can be found from Eq. (60). Since the angular momentum L only enters squared in the Hamiltonian constraint (60), the conformal factor ψ is even in L . In general, a solution to this quasi-linear elliptic equation has to be constructed numerically, but an approximate solution up to $O(L^4)$ is given by

$$\psi = 1 + \frac{M}{2r} + \left(\frac{L}{M^2}\right)^2 \left(1 + \frac{M}{2r}\right)^{-5} \left[\tilde{\psi}_0 + \tilde{\psi}_2 P_2(\cos \theta)\right] + F(r, \theta) L^4 \quad (63)$$

where

$$\tilde{\psi}_0 = -\frac{M}{5r} \left[5 \left(\frac{M}{2r}\right)^3 + 4 \left(\frac{M}{2r}\right)^4 + \left(\frac{M}{2r}\right)^5\right] \quad (64)$$

and

$$\tilde{\psi}_2 = -\frac{1}{10} \left(\frac{M}{r}\right)^3 \quad (65)$$

and where the $P_2(\cos \theta) = (3 \cos^2 \theta - 1)/2$ is the second Legendre polynomial (see GNPP.) We allow for an *unknown* $O(L^4)$ contribution by including the unknown function $F(r, \theta)$ that, in principle, can be found by solving the Hamiltonian constraint to $O(L^4)$ in a method similar to that of GNPP.

The extrinsic curvature, which must be odd in L , can then be found from Eq. (59)

$$\begin{aligned} K_{r\phi} &= \psi^{-2} \bar{A}_{r\phi} \\ &= 12 \frac{\sin^2 \theta}{(2r + M)^2} L - \frac{48}{5} \frac{[8(1 - 3 \cos^2 \theta)r^3 - 20Mr^2 - 8M^2r - M^3] \sin^2 \theta}{(2r + M)^8} L^3 + O(L^5). \end{aligned} \quad (66)$$

Even though we will find the BB radiation scalar ξ is of order $O(L^4)$, it turns out that it depends only on terms in ψ up to order $O(L^2)$, so that it is independent of the unknown function $F(r, \theta)$. A heuristic argument for this behavior can be given as follows (for a more rigorous proof see Appendix D.) The Bowen–York solution is equivalent to the Kerr solution up to $O(L)$, and deviations enter only at order $O(L^2)$. In a transverse frame we therefore expect the leading-order terms in the Weyl scalars ψ_0 and ψ_4 , which are measures of the gravitational radiation that is absent in the Kerr solution, to be $O(L^2)$. The leading order term in the radiation scalar ξ , being the product of ψ_0 and ψ_4 should therefore be $O(L^4)$, and higher order corrections in the conformal factor should enter at higher order.

To construct ξ , we first compute the electric (3) and magnetic (7) parts of the Weyl tensor. We list the results in Appendix C, and point out that these quantities do depend on $F(r, \theta)$. We then compute the matrix C^i_j and, using (9) and (10), the invariants I (C14) and J (C15). Again, I, J depend on $F(r, \theta)$. From (11) we find the speciality index S to $O(L^4)$

$$S = 1 - \frac{3^3 2^{10}}{5^2} \frac{(4r^2 - 21Mr + M^2)^2 r^4 \sin^4 \theta}{M^4 (2r + M)^{12}} L^4, \quad (67)$$

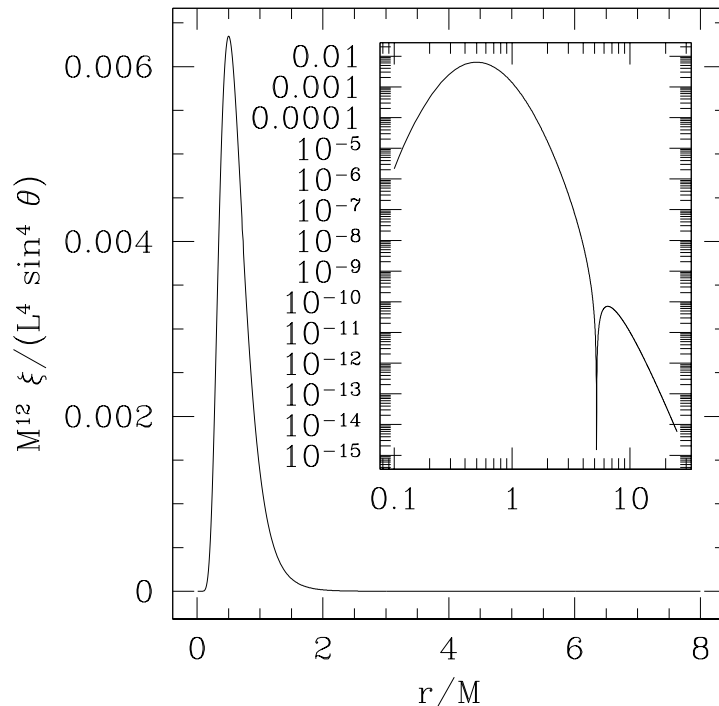


FIG. 2: The dimensionless BB scalar $M^{12}\xi/(L^4 \sin^4 \theta)$ for Bowen–York initial data as a function of r/M . (For $\theta = 0, \pi$, the BB scalar $\xi = 0$.)

which turns out to be independent of $F(r, \theta)$. Because we were able to express the speciality index as a deviation from unity—i.e., we expressed spacetime as a deviation from algebraic speciality—we can find the BB scalar ξ immediately from (17) to $O(L^4)$

$$\xi = \frac{3^2 2^{22}}{5^2} \frac{(4r^2 - 21Mr + M^2)^2 r^{10} \sin^4 \theta}{M^2 (2r + M)^{24}} L^4 \quad (68)$$

(see Fig. 2). To $O(L^2)$ the Coulomb scalar χ is given by

$$\begin{aligned} \chi = & -64 \frac{Mr^3}{(2r + M)^6} - 768 i \cos \theta \frac{r^4}{(2r + M)^8} L + \frac{768}{5} (24r^4 + 8r^4 \cos^2 \theta + 24r^3 M \cos^2 \theta \\ & - 8Mr^3 + 2r^2 M^2 \cos^2 \theta - 14M^2 r^2 - 8M^3 r - M^4) \frac{r^3}{M(2r + M)^{12}} L^2. \end{aligned} \quad (69)$$

As expected, the BB radiation scalar scales with L^4 . Since the deviation between Bowen–York data and a Kerr spacetime enters at order L^2 , the amplitude of the emitted gravitational radiation also scales with L^2 , and the power carried by the gravitational waves accordingly with L^4 (see GNPP.) As we have seen for the linearized waves on flat backgrounds in Section III, the BB radiation scalar scales with the square of the gravitational wave amplitude. At great distances ($r \gg M$), the BB scalar $\xi \sim L^4/(M^2 r^{10})$. The peeling off of the BB scalar with r^{-10} is understood as follows: The BB scalar is expected to drop like the product of ψ_0 and ψ_4 . The usual peeling off of the product is expected to scale like M^2/r^6 . However, in the Kerr spacetime at that order it would be multiplied by a *zero* coefficient. The next order, which would peel off like L^2/r^8 , also vanishes because the deviation of the Bowen–York initial data from Kerr is at second-order in L in the metric functions. The next term is indeed the one found. This scaling is quadratic in $\chi - \chi_{\text{Kerr}}$, as expected. When ξ is calculated by finding the difference between I and χ^2 , the Kerr contributions to χ cancel with the Kerr contributions to I , so that the BB scalar ξ depends only on the radiative Bowen–York degrees of freedom.

Notice, that ξ peaks at $r = M/2$, i.e., at the Schwarzschild black hole’s event horizon. The radiation described by the BB scalar inside the event horizon evidently cannot change the exterior spacetime. However, because the greatest deviations of the Bowen–York initial data from Kerr are localized near the event horizon, it is expected that much of this spurious radiation be absorbed by the black hole.

V. KASNER SPACETIME

The Kasner spacetime is a homogeneous vacuum spacetime. From its spacetime metric we identify a unity lapse, a vanishing shift vector, and the spatial metric

$$d\sigma^2 = t^{2p_1} dx^2 + t^{2p_2} dy^2 + t^{2p_3} dz^2, \quad (70)$$

where the parameters p_i satisfy $p_1 + p_2 + p_3 = 1 = p_1^2 + p_2^2 + p_3^2$. It is convenient express p_2 and p_3 in terms of p_1 , which we will call p , so that

$$p \equiv p_1 \quad p_{2,3} = (1 - p \pm \varrho)/2, \quad (71)$$

where $\varrho = [(1-p)(1+3p)]^{1/2}$. The Kasner spacetime is sufficiently simple to construct the BB radiation scalar in closed form, and also to demonstrate the construction of the quasi-Kinnersley frame from spatial data as they are used in numerical relativity.

We compute the extrinsic curvature from the spatial metric and find

$$K_{ab} = \text{diag}[-p t^{2p-1}, -(1-p+\varrho) t^{-p+\varrho}/2, -(1-p-\varrho) t^{-p-\varrho}/2], \quad (72)$$

so that $K = -1/t$. For the Kasner spacetime the magnetic part of the Weyl tensor vanishes, so that $C_{ab} = E_{ab}$. The only non-vanishing components are

$$\begin{aligned} C^x_x &= p(1-p)t^{-2} \\ C^y_y &= (1-p+\varrho)(1+p-\varrho)t^{-2}/4 \\ C^z_z &= (1-p-\varrho)(1+p+\varrho)t^{-2}/4, \end{aligned} \quad (73)$$

From (9) and (10) we now find the Weyl tensor invariants

$$I = \frac{p^2(1-p)}{t^4} \quad (74)$$

$$J = \frac{p^4(1-p)^2}{2t^6}, \quad (75)$$

and from (11) the speciality index

$$S = \frac{27}{4}(1-p)p^2. \quad (76)$$

Since the matrix C^a_b is diagonal, its three eigenvalues and corresponding eigenvectors can be found quite easily. In order to find which one of these corresponds to the quasi-Kinnersley frame we parametrize p as $p = -1/3 + q$ where q does not need to be small. Inserting this into (76) we find

$$S - 1 = -\frac{27}{4}q + \frac{54}{4}q^2 - \frac{27}{4}q^3. \quad (77)$$

The case $q = 0$ corresponds to an algebraically special spacetime (Petrov type D), and for small values of q we can therefore use the expansion (16) to find

$$\chi = -\frac{2}{9t^2} \left(1 - \frac{15}{4}q + \frac{9}{4}q^2 + \dots \right) \quad (78)$$

For small values of q this coincides with $\lambda_x/2$, so that we can identify

$$\chi = -\frac{p_2 p_3}{2t^2}. \quad (79)$$

We can find the BB scalar ξ either from the series expansion (17), or, having found χ already, from (15), which yields

$$\xi = \frac{q}{9t^4} (1-3q)^2 \left(1 - \frac{3}{4}q \right) = \frac{1}{4t^4} p_1^2 (p_2 - p_3)^2. \quad (80)$$

Evidently we have $\xi \neq 0$, even though no radiation is present in the Kasner spacetime. [There are three cases for which $\xi = 0$: $q = 0$ (spacetime is Petrov type D), and $q = 1/3$ or $4/3$, which are flat spacetimes (Petrov type 0).] While this seems very counter-intuitive, we remind the reader that the BB radiation scalar is an unambiguous measure of gravitational radiation *only* in a radiation zone, which the homogeneous Kasner solution does not possess. The *name* “radiation scalar” is therefore may be misleading in this case.

Our results for I, J , and χ for the Kasner spacetime agree with those obtained through a pure spacetime approach by Cherubini *et al.* [20], who also compute the Weyl scalars ψ_0 and ψ_4 in a transverse frame, and their product agrees with our value of ξ , as expected.

We now demonstrate how the quasi-Kinnersley frame can be constructed from spatial data. The eigenvector that corresponds to the eigenvalue λ_x , and hence to the quasi-Kinnersley frame, is

$$\hat{\sigma}^a = s \delta_x^a, \quad (81)$$

where $s = t^{-p_1}$ is a normalization constant. Evidently $\hat{\sigma}^a$ is real and has vanishing imaginary part.

Following paper I, the two real projections onto the hypersurface of the two real null vectors of the spacetime tetrad are

$$\hat{\lambda}^a = t^{-p_1} \delta_x^a \quad \hat{\nu}^a = -t^{-p_1} \delta_x^a, \quad (82)$$

so that, with the unit normal to the hypersurface $\hat{\tau}^a = \delta_t^a \partial_a$, the two real spacetime null vectors of the frame are, up to a spin-boost parameter c , given by

$$\ell^a = \frac{|c|}{\sqrt{2}} (\partial_t + t^{-p_1} \partial_x) \quad (83)$$

$$n^a = \frac{|c|^{-1}}{\sqrt{2}} (\partial_t - t^{-p_1} \partial_x). \quad (84)$$

Notice, that the two real projections of ℓ^a, n^a on the hypersurface are anti-parallel. This happens because by construction the normal $\hat{\tau}^a$ lies in the spacetime tangent 2-plane spanned by ℓ^a and n^a . In this degenerate case, the complex basis vector m^a can be found as follows (see paper I for details). We first choose an arbitrary real unit vector \hat{r}^a in the spatial 2-plane orthogonal to $\hat{\lambda}^a = -\hat{\nu}^a$. Then,

$$m^a = \frac{e^{i\vartheta}}{\sqrt{2}} \left(\hat{r}^a + i \varepsilon^{abc} \hat{\lambda}_b \hat{r}_c \right). \quad (85)$$

We find that $\varepsilon^{abc} = -[a b c] / \sqrt{\det(g_{mn})} = -[a b c] / t$, with $[a b c]$ being the permutation symbol. We next choose $\hat{r}^a = t^{-p_2} \delta_y^a$, so that

$$m^a = \frac{e^{i\vartheta}}{\sqrt{2}} \left(t^{-p_2} \partial_y - i t^{-p_3} \partial_z \right). \quad (86)$$

The vectors (83),(84), and (86) are the vectors that make the quasi-Kinnersley frame. Note that we are able to determine the quasi-Kinnersley frame only up to spin-boost with parameter $c = |c| \exp(i\vartheta)$. In some situations one can choose the spin-boost parameter based on the physical properties of spacetime, so that the quasi-Kinnersley tetrad can be found (see, e.g., Ref. [21]). However, this problem awaits further study.

VI. SUMMARY AND DISCUSSION

The BB radiation scalar ξ was introduced as an invariant measure of gravitational radiation in regions of spacetime where such radiation is unambiguously defined. However, it is uniquely and smoothly extended throughout a generic spacetime. In this paper, we have computed ξ for a variety of analytical spacetimes and initial data sets, adopting a formalism that relies only on spatial data as they are typically used in numerical relativity. These calculations have illustrated the procedure used to define ξ explicitly. That procedure has been described previously [8, 9, 10], but not implemented. Its actual implementation here, therefore, should help clarify the procedure in general.

For those examples we have considered here which unambiguously contain gravitational radiation, namely linearized waves on flat backgrounds and Bowen–York initial data for rotating black holes, our radiation scalar scales with the square of parameters that govern the gravitational wave amplitude. This suggests that it does indeed provide a

reasonable measure of the gravitational wave content of these data. (The speciality index S , in contrast, is independent of the waves' amplitude when the Coulombic part of curvature is perturbative.) We also have examined the homogeneous, cosmological Kasner solutions. In this case we found a non-vanishing ξ even though Kasner does not contain gravitational radiation. We explain this apparent contradiction by noting the absence of a radiation zone in the Kasner spacetime. Thus, although the name “radiation scalar” for ξ is misleading and inappropriate in this case, ξ can still be found uniquely. From the mathematical point of view, it remains an interesting gauge-invariant “observable” even when it is not a *radiation* scalar.

This paper has illustrated the potential of ξ as a tool for discriminating among initial data sets for numerical relativity. However, it has done so using analytic, rather than actual numerical, data. An actual application to such numerical data sets would engender a fresh set of difficulties, originating in the fundamental discreteness of the variables involved and the associated subtlety in obtaining the required *smooth* extension of the quasi-Kinnersley frame into the strong-field regions of the initial data set. A full discussion of these issues lies outside the scope of this paper, and will be addressed elsewhere. However, we must make some comment here. To illustrate the resolution we envision to these difficulties in actual numerical work, we examine the results of Figure 3 in the Appendix. These figures show all three values of the Coulomb and BB scalars, appropriately scaled to give dimensionless quantities, for linearized Einstein–Rosen waves of flat spacetime. At large radii, one branch of the upper graph, the dotted one, is clearly larger than the other two. This is the principal branch of ξ , and is associated with the quasi-Kinnersley frame in this region. Moving inward, there are three critical points where we must be careful, at $\rho/a = \sqrt{2}$, 1 and $1/\sqrt{2}$.

The outermost critical point poses no real problem since the root we had been tracking, ξ^0 , is visibly discontinuous there. If we were moving inward in a numerical spacetime, calculating eigenvalues of the tensor C^i_j with sufficiently small radial steps, there is no way we would be confused about which eigenvalue was appropriate just inside $\rho/a = \sqrt{2}$. Inside this first critical point, we would naturally be tracking the dashed root, rather than the dotted.

The next critical point, at $\rho/a = 1$ poses a greater difficulty. The discontinuity there occurs in the derivative of the Coulomb scalar, rather than in the scalar itself, and could therefore be harder to detect in numerical data. However, even in this case, there is a simple resolution to the problem. We would be able to recognize numerically that the eigenvalue we are interested in, associated with the dashed curve, is degenerating with another, associated with the solid curve. There are then at least two things we could do to make sure the Coulomb scalar remains smooth at this critical point. One would be to use higher-order approximants, such as splines based on χ -values at several grid points in each direction around the critical point, to explore which branch we ought to pick to preserve smoothness. An even simpler approach would be to exploit the known analytic structure of the Riemann surface underlying the multi-valued complex function underlying χ . That structure is described in detail in Papers I and II. Essentially, this approach would boil down to calculating how the speciality index S varies in a neighborhood of the critical point, and mapping spacetime in that neighborhood into the Riemann surface. The critical point itself occurs where S lies exactly on the branch line we have chosen for χ . As S crosses that branch line, there is no ambiguity at this level in how the branch of χ ought to change to preserve analyticity. Thus, once we have detected the possible presence of such a critical point in numerical data, we could use the explicit formula of (12) and the local structure of the function S on spacetime to predict the exact eigenvalue which corresponds to the quasi-Kinnersley frame at every grid-point nearby.

The third critical point, at $\rho/a = 1/\sqrt{2}$ poses no difficulty whatsoever. At this point, the quasi-Kinnersley value is associated with the solid curve, and it is the other two which are discontinuous. We would scarcely notice this in actual numerical work.

The Einstein–Rosen example discussed here is actually quite useful. The three critical points we have observed in this example typify the only three kinds of critical points which can occur in a general spacetime, whether numerical or analytic in origin. The above discussion shows how these three types of critical point may be handled using a combination of simple numerical tests and insights from the analytical development of the radiation scalar approach. Although further testing will doubtless be required in developing general numerical implementations, these observations are encouraging for the ultimate viability of this approach in numerical relativity.

A second question which lies outside the scope of the present paper, but which we nonetheless ought to address briefly here, concerns how the radiation scalar could potentially be used in discriminating among potential choices of initial data. Consider, for example, initial data describing a compact binary at small binary separation. As we have discussed before, these data will presumably contain “astrophysically sound” radiation together with the “junk radiation” that we would like to minimize. Such initial data can be constructed using different approaches, namely different decompositions of the constraint equations and different choices for the freely specifiable background geometry. Different choices lead to physically distinct solutions [1, 6, 7] with distinct gravitational wave content. Our comparison of Kerr and Bowen–York data for rotating black holes in Section IV illustrates how the BB radiation scalar may be used as a diagnostic for comparing the amount of gravitational waves that these initial data sets would emit when evolved dynamically.

We find in the analytical examples considered here that the BB radiation scalar scales as expected with a parameter

that controls the gravitational wave content of these examples. Such a parameter may not exist in numerically generated initial data sets, in which case it may be less clear how any non-zero value of ξ should be interpreted. The BB radiation scalar may nevertheless be a useful diagnostic. Even for a single initial data set the ratio ξ/χ^2 would provide a dimensionless measure of the strength of the “radiative” fields compared to the “coulombic” fields. Perhaps more importantly, it may be useful to compare ξ for different initial data sets that approximate the same physical situation. For example, such a comparison may provide some guidance for deciding which choices in the construction of initial data sets yields a more truthful representation of binary black holes or neutron stars at small binary separations. We can envision various different ways of how such a comparison could be made. One potentially useful approach would focus on the radiation zone, where we have reliable intuition about how the real radiation content ought to fall off. Comparing the fall-off behavior with that of the BB radiation scalar may help distinguish this “astrophysically sound” radiation content from the “junk” content and minimize the latter.

As a word of caution, however, we point out that such a comparison can at best provide some guidance rather than conclusive evidence. It is possible that the individual radiation fields ψ_0 and ψ_4 change in such a way that their product $\xi = \psi_0\psi_4$ decreases even though the true radiation content increases. However, for many generic sets (or families) of initial data this may not be the case. Since a diagnostic providing conclusive evidence is not yet available, we therefore believe that the BB radiation scalar may in the meantime provide some useful guidance as long as we keep these caveats in mind.

We finally discuss some further limitations of this approach. While the BB radiation scalar ξ contains some measure of gravitational wave content, it is not clear immediately how this information can be translated into gravitational wave templates that might be useful for gravitational wave observers. Specifically such observers would presumably measure the gravitational wave amplitudes h_\times and h_+ in a transverse-traceless frame. In the linearized examples we have studied here, both the intuitive gravitational wave content and the BB radiation scalar scales with the square of a parameter describing intuitively the strength of the waves being modeled. This does not mean, however, that ξ is proportional to the energy of the gravitational wave. In general the latter scales with $|\psi_0 + \psi_4|^2$ in the appropriate basis, while $\xi = \psi_0\psi_4$. Since ψ_0 and ψ_4 have different fall-off behavior, ξ also falls off differently from both the gravitational wave amplitude or energy. In short, although ξ describes only the radiative degrees of freedom, ξ does not carry with it *all* the information—or even sufficient information—about the gravitational waves required by observers. This issue will be discussed more fully in a forthcoming paper.

Acknowledgments

The authors are indebted to Marco Bruni and Andrea Nerozzi for invaluable discussions. TWB gratefully acknowledges support from the J. S. Guggenheim Memorial Foundation. This work was supported in part by NSF Grant PHY-0139907 to Bowdoin College, by NSF grant PHY-0400588 to Florida Atlantic University, and by NASA grant ATP03-0001-0027 through the University of Texas at Brownsville.

APPENDIX A: DIRECT CALCULATION FOR EINSTEIN-ROSEN WAVES

In this appendix we find χ and ξ for Einstein-Rosen cylindrical waves directly from Eqs. (12) and (13). First, we re-write Eq. (12) as

$$\chi^{0,\pm} = -\frac{3}{2} \frac{J}{I} Z_\chi^{0,\pm}(S), \quad (\text{A1})$$

where

$$Z_\chi^i(S) = \frac{1}{\sqrt{S}} \left[\alpha_i \left(\sqrt{S} - \sqrt{S-1} \right)^{1/3} + \alpha_i^{-1} \left(\sqrt{S} - \sqrt{S-1} \right)^{-1/3} \right] \quad (\text{A2})$$

Here, α is one of the three cubic roots of unity, $\alpha_0 = 1$, $\alpha_+ = \exp(2i\pi/3)$, and $\alpha_- = \exp(4i\pi/3)$. By the cubic and square roots in Eq. (A2) we mean the principal branch roots for either. The choice of the cubic root then is done through the choice of α_i . This choice labels the three different branches of the function $Z_\chi^i(S)$. The corresponding functions $\xi^{0,\pm}$ can be calculated using

$$\xi^{0,\pm} = I - 3(\chi^{0,\pm})^2, \quad (\text{A3})$$

or, equivalently, from Eq. (13) using a similar approach to its three branches.

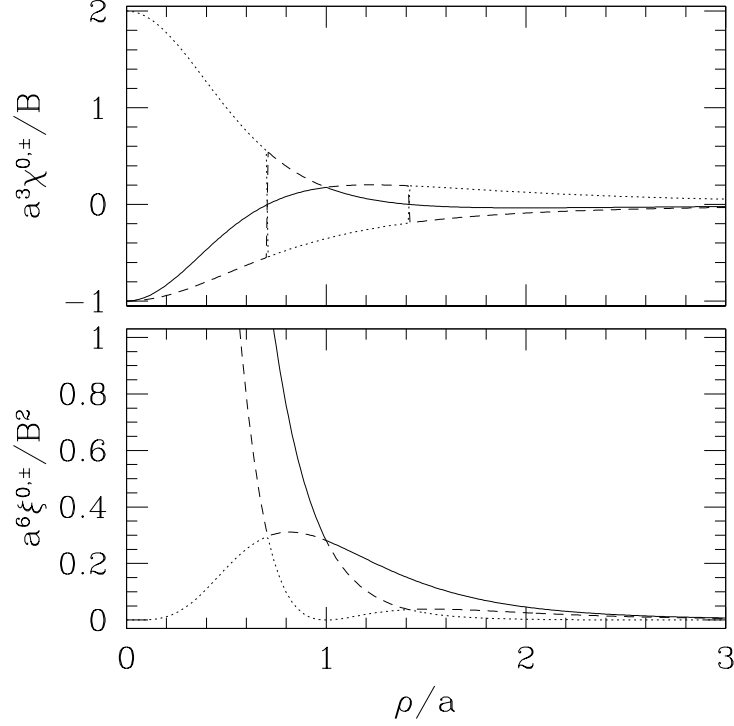


FIG. 3: The three branches of the Coulomb scalar $\chi^{0,\pm}$ (top panel) and the BB scalar $\xi^{0,\pm}$ (bottom panel) for linearized Einstein–Rosen cylindrical waves. The principal branch— χ^0 and ξ^0 —are dotted, χ^- and ψ^- are dashed, and χ^+ and ψ^+ are the solid curves.

Figure 3 shows the three different branches for $\chi^{0,\pm}$ and $\xi^{0,\pm}$, correspondingly. Notice that the three branches for either function are non-differentiable, and for χ^0 and χ^- even discontinuous. For either function, however, branches can be changed so that the resulting functions are smooth. The identity of the physically meaningful functions can be determined by demanding a proper asymptotic behavior of χ and ξ . In this case, starting at great distances, the chosen branch is the principal branch, χ^0 (and correspondingly, ξ^0). At the branch point $\rho/a = \sqrt{2}$ we change the branch to χ^- (and, correspondingly, ξ^-), and at $\rho/a = 1$ we change the branch to χ^+ (and, correspondingly, ξ^+). The resulting *smooth* curves are identical with those presented in Fig. 1.

APPENDIX B: SOME EXPRESSIONS FOR LINEARIZED QUADRUPOLE WAVES

From the spatial Ricci tensor we find that at the moment of time symmetry, $t = 0$, the only non-vanishing components of C_j^i are to leading order in ϵ ,

$$C_r^r = 24(25r^6\lambda^3 - 2r^8\lambda^4 + 54r^2\lambda - 78r^4\lambda^2 + 224r^4\lambda^2\cos^2\theta - 73r^6\lambda^3\cos^2\theta - 158r^2\lambda\cos^2\theta + 6r^8\lambda^4\cos^2\theta + 4\cos^2\theta)e^{-r^2\lambda}\epsilon/r^2 \quad (\text{B1})$$

$$C_r^\theta = r^{-2}C_\theta^r = 24\sin\theta\cos\theta(-12 + 293r^6\lambda^3 - 64r^8\lambda^4 + 150r^2\lambda + 4r^{10}\lambda^5 - 420r^4\lambda^2)e^{-r^2\lambda}\epsilon/r^3 \quad (\text{B2})$$

$$C_\theta^\theta = -24(6 + 715r^6\lambda^3 - 290r^8\lambda^4 + 78r^2\lambda + 292r^8\lambda^4\cos^2\theta - 739r^6\lambda^3\cos^2\theta - 567r^4\lambda^2 + 640r^4\lambda^2\cos^2\theta + 43r^{10}\lambda^5 - 43\cos^2\theta r^{10}\lambda^5 - 130r^2\lambda\cos^2\theta - 4\cos^2\theta - 2r^{12}\lambda^6 + 2\cos^2\theta r^{12}\lambda^6)e^{-r^2\lambda}\epsilon/r^2 \quad (\text{B3})$$

$$C_\phi^\phi = 24(6 + 690r^6\lambda^3 - 288r^8\lambda^4 + 24r^2\lambda + 286r^8\lambda^4\cos^2\theta - 666r^6\lambda^3\cos^2\theta - 489r^4\lambda^2 + 416r^4\lambda^2\cos^2\theta + 43r^{10}\lambda^5 - 43\cos^2\theta r^{10}\lambda^5 + 28r^2\lambda\cos^2\theta - 8\cos^2\theta - 2r^{12}\lambda^6 + 2\cos^2\theta r^{12}\lambda^6)e^{-r^2\lambda}\epsilon/r^2, \quad (\text{B4})$$

Restricting analysis to the equatorial plane, $\theta = \pi/2$, we find the curvature scalars

$$I = 576(36 - 1548 r^4 \lambda^2 - 51744 r^6 \lambda^3 + 353559 r^8 \lambda^4 - 27664 r^{18} \lambda^9 - 172 r^{22} \lambda^{11} - 451732 r^{14} \lambda^7 + 612 r^2 \lambda - 773889 r^{10} \lambda^5 + 803755 r^{12} \lambda^6 + 3005 r^{20} \lambda^{10} + 146051 r^{16} \lambda^8 + 4 r^{24} \lambda^{12}) e^{-2r^2 \lambda} \epsilon^2 / r^4 \quad (\text{B5})$$

and

$$J = -6912 \lambda (2 r^6 \lambda^3 - 54 + 78 r^2 \lambda - 25 r^4 \lambda^2) \times (-6 - 690 r^6 \lambda^3 + 288 r^8 \lambda^4 - 24 r^2 \lambda - 43 r^{10} \lambda^5 + 489 r^4 \lambda^2 + 2 r^{12} \lambda^6) \times (-6 - 715 r^6 \lambda^3 + 290 r^8 \lambda^4 - 78 r^2 \lambda - 43 r^{10} \lambda^5 + 567 r^4 \lambda^2 + 2 r^{12} \lambda^6) e^{-3r^2 \lambda} \epsilon^3 / r^4 \quad (\text{B6})$$

From these we compute the speciality index

$$S = 27 r^4 \lambda^2 (2 r^6 \lambda^3 - 54 + 78 r^2 \lambda - 25 r^4 \lambda^2)^2 (-6 - 690 r^6 \lambda^3 + 288 r^8 \lambda^4 - 24 r^2 \lambda - 43 r^{10} \lambda^5 + 489 r^4 \lambda^2 + 2 r^{12} \lambda^6)^2 \times (-6 - 715 r^6 \lambda^3 + 290 r^8 \lambda^4 - 78 r^2 \lambda - 43 r^{10} \lambda^5 + 567 r^4 \lambda^2 + 2 r^{12} \lambda^6)^2 / [4(36 - 1548 r^4 \lambda^2 - 51744 r^6 \lambda^3 + 353559 r^8 \lambda^4 - 27664 r^{18} \lambda^9 - 172 r^{22} \lambda^{11} - 451732 r^{14} \lambda^7 + 612 r^2 \lambda - 773889 r^{10} \lambda^5 + 803755 r^{12} \lambda^6 + 3005 r^{20} \lambda^{10} + 146051 r^{16} \lambda^8 + 4 r^{24} \lambda^{12})^3] . \quad (\text{B7})$$

As expected, S is independent of the wave amplitude ϵ . Note, that for $\lambda r^2 \rightarrow \infty$, $S \rightarrow 0$. This is in spite of the fact that spacetime approaches algebraic speciality. In fact, spacetime approaches algebraic speciality exponentially fast, as both I and J decay exponentially with λr^2 . This behavior is captured by the BB scalar ξ : from Eq. (13), ξ equals I times a function of S only. The speciality index S is dropping off at great distances to zero like $\lambda^{-4} r^{-8}$, so that the function that multiplies I approaches a constant. The BB scalar ξ drops off exponentially, specifically like $\exp(-2\lambda r^2)$.

Figure 4 shows the speciality index S as a function of $\lambda^{1/2} r$ on the equatorial plane. There are 15 values of r for which $S = 1$, arranged in five triplets. The values of $\rho = \lambda^{1/2} r$ for which $S = 1$ are

$$\begin{aligned} 1\rho_{1,2,3} &= 0.30800524515557994139, & 0.45049403784384619791, & 0.59829320761717622144 \\ 2\rho_{1,2,3} &= 1.0335527869353531668, & 1.0467779593567221747, & 1.0682855799176748686 \\ 3\rho_{1,2,3} &= 1.6984496413703925629, & 1.7168422939913076313, & 1.7311171061162415883 \\ 4\rho_{1,2,3} &= 2.4478787994829345025, & 2.4658595692782475639, & 2.4824885271217855892 \\ 5\rho_{1,2,3} &= 3.3409626177591728790, & 3.3526507427990501828, & 3.3643720160172523032 \end{aligned} \quad (\text{B8})$$

In between points at which $S = 1$, we have points at which $|S - 1| = 1$, which occur at the following locations:

$$\begin{aligned} 1\rho_{1,2,3}^* &= 0, & 0.39945741403776425339, & 0.50160586730815486639 \\ 2\rho_{1,2,3}^* &= 0.98542263099668675629, & 1.0416944916187449946, & 1.0527498193777135990 \\ 3\rho_{2,3}^* &= & 1.7112566884721670706, & 1.7219786282054512104 \\ 4\rho_{1,2,3}^* &= 1.8534934086232694765, & 2.4600232831874878020, & 2.4715457963797601620 \\ 5\rho_{1,2,3}^* &= 2.8449085086360266876, & 3.3487504415432614190, & 3.3565547217000555743 \end{aligned} \quad (\text{B9})$$

Notice that there is no value for $3\rho_1^*$: the speciality index S does not vanish between $2\rho_3$ and $3\rho_1$. In addition, $|S - 1| \rightarrow 1$ also as $\lambda^{1/2} r \rightarrow \infty$.

It appears that in some cases – specifically for odd-parity quadrupole waves – the curvature invariant J may vanish to $O(\epsilon^3)$, so that its leading order is $O(\epsilon^4)$. Generic gravitational waves include both polarization states, so that the total curvature invariant J is still of $O(\epsilon^3)$, and $S = O(\epsilon^0)$.

APPENDIX C: RESULTS FOR BOWEN–YORK INITIAL DATA

Inserting (66) into

$$\mathcal{B}_{ij} = -\epsilon_i^{kl} \nabla_k K_{lj} = -\gamma_{im} \epsilon^{mkl} (K_{lj,k} - K_{ln} \Gamma_{jk}^n) \quad (\text{C1})$$

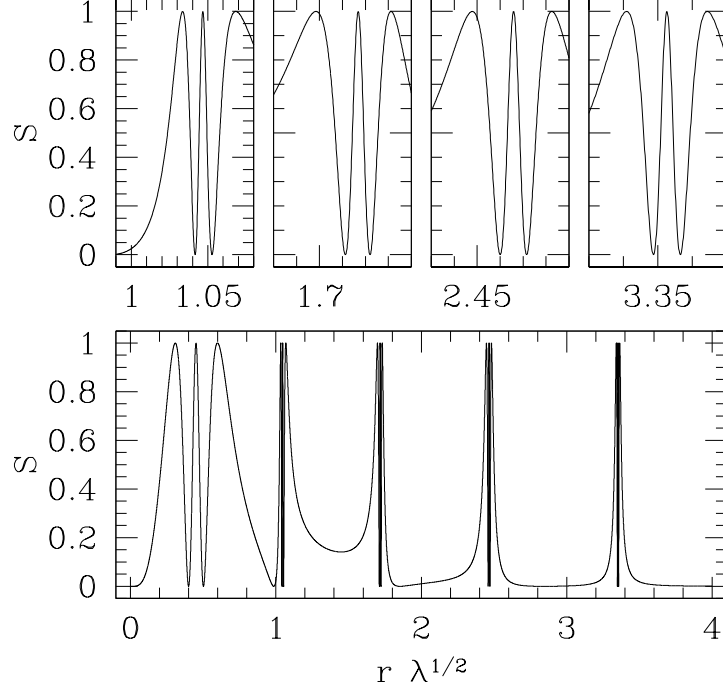


FIG. 4: The speciality index S as a function of $\lambda^{1/2} r$ on the equatorial plane, for linearized, even-parity, quadrupole waves. The top panel magnifies the regions where S oscillates rapidly.

and symmetrizing we find that the only non-vanishing coefficients of the magnetic part of the Weyl tensor are

$$B_{rr} = -\frac{64 \cos \theta}{(2r + M)^4} L + \frac{1536 [16(2 - 3 \cos^2 \theta)r^3 - 20Mr^2 - 8M^2r - M^3] \cos \theta}{10 M (2r + M)^{10}} L^3 \quad (\text{C2})$$

$$B_{r\theta} = -\frac{48 r (2r - M) \sin \theta}{(2r + M)^5} L + \frac{384 [40(1 - 3 \cos^2 \theta)r^4 - 20(7 - 3 \cos^2 \theta)Mr^3 - 16M^2r^2 + 4M^3r + M^4] r \sin \theta}{5 (2r + M)^{11}} L^3 \quad (\text{C3})$$

$$B_{\theta\theta} = 48 \frac{\cos \theta r^2}{(2r + M)^4} L + \frac{384 \cos \theta [20 M r^2 + 8 M^2 r + M^3 + 24 r^3 \cos^2 \theta - 8 r^3] r^2}{5 (2r + M)^{10} M} L^3 \quad (\text{C4})$$

$$B_{\phi\phi} = 48 \frac{\cos \theta \sin^2 \theta r^2}{(2r + M)^4} L + \frac{384 \cos \theta \sin^2 \theta [72 r^3 \cos^2 \theta - 56 r^3 + 20 M r^2 + 8 M^2 r + M^3] r^2}{5 (2r + M)^{10} M} L^3 \quad (\text{C5})$$

The electric part of the Weyl tensor is computed from the Ricci tensor, whose non-vanishing components to $O(L^4)$

are

$$\begin{aligned}
R_{rr} = & -\frac{8M}{(2r+M)^2 r} \\
& + \frac{32}{5} \frac{144r^4 \cos^2 \theta - 360r^3 M \cos^2 \theta + 36r^2 M^2 \cos^2 \theta - 32M^2 r^2 - 48r^4 - 8M^3 r + 440Mr^3 - M^4}{(2r+M)^8 M r} L^2 \\
& + \frac{64}{25} [-8896Mr^6 + 16176M^2r^5 + 6480M^3r^4 + 800M^4r^3 - 36M^5r^2 - 12rM^6 - M^7 + 960r^7 \\
& - 10704r^5 \cos^2 \theta M^2 + 31872r^6 \cos^2 \theta M - 14400Mr^6 \cos^4 \theta + 2016M^2r^5 \cos^4 \theta - 240M^4r^3 \cos^2 \theta \\
& + 36M^5r^2 \cos^2 \theta - 3360r^4 \cos^2 \theta M^3 - 5184r^7 \cos^2 \theta + 8064r^7 \cos^4 \theta] L^4 / [(2r+M)^{14} M^2 r] \\
& + \frac{4L^4}{2r+M} \left[\frac{2M(2r-M)}{r(2r+M)^2} - \frac{\cot \theta}{r} \partial_\theta - 2 \frac{2r+3M}{2r+M} \partial_r - \frac{1}{r} \partial_{\theta\theta} - 2r \partial_{rr} \right] F(r, \theta) \tag{C6}
\end{aligned}$$

$$\begin{aligned}
R_{r\theta} = & \frac{768}{5} \sin \theta \cos \theta \frac{r^2 (2r-M)}{(2r+M)^7 M} L^2 \\
& + \frac{1536}{25} r^2 \sin \theta \cos \theta (156r^4 \cos^2 \theta - 52r^4 - 78r^3 M \cos^2 \theta + 186Mr^3 + 26M^2r^2 \\
& - 3M^3r - M^4) L^4 / [(2r+M)^{13} M^2] + \frac{4}{2r+M} L^4 \left(2 \frac{r-M}{2r+M} \partial_\theta - r \partial_{r\theta} \right) F(r, \theta) \tag{C7}
\end{aligned}$$

$$\begin{aligned}
R_{\theta\theta} = & \frac{4Mr}{(2r+M)^2} \\
& - \frac{16}{5} \frac{(168r^4 \cos^2 \theta - 72r^4 - 304Mr^3 + 384r^3 M \cos^2 \theta + 42r^2 M^2 \cos^2 \theta - 38M^2 r^2 - 8M^3 r - M^4)r}{(2r+M)^8 M} L^2 \\
& - \frac{32}{25} (1152r^7 - M^7 - 3424Mr^6 + 1152M^2r^5 + 384M^3r^4 - 42M^5r^2 - 12M^6r + 8M^4r^3 + 13284r^7 \cos^4 \theta \\
& - 11136r^7 \cos^2 \theta + 8640r^6 M \cos^4 \theta + 3360r^6 M \cos^2 \theta + 3456r^5 M^2 \cos^4 \theta + 2880r^5 M^2 \cos^2 \theta + 2736r^4 M^3 \cos^2 \theta \\
& + 552r^3 M^4 \cos^2 \theta + 42r^2 M^5 \cos^2 \theta) r L^4 / [M^2 (2r+M)^{14}] \\
& - \frac{4r}{2r+M} L^4 \left[\frac{M(2r-M)}{(2r+M)^2} + \cot \theta \partial_\theta + \frac{r(6r+M)}{2r+M} \partial_r + 2 \partial_{\theta\theta} + r^2 \partial_{rr} \right] F(r, \theta) \tag{C8}
\end{aligned}$$

$$\begin{aligned}
R_{\phi\phi} = & \frac{4Mr}{(2r+M)^2} \sin^2 \theta \\
& - \frac{16}{5} \sin^2 \theta \frac{(336r^3 M \cos^2 \theta + 30r^2 M^2 \cos^2 \theta + 120r^4 \cos^2 \theta - 24r^4 - 8M^3 r - 256Mr^3 - 26M^2 r^2 - M^4)r}{M(2r+M)^8} L^2 \\
& - \frac{32}{25} \sin^2 \theta (1440M^2r^5 \cos^4 \theta + 576Mr^6 \cos^4 \theta + 5760r^7 \cos^4 \theta + 408M^4r^3 \cos^2 \theta \\
& - 2688r^7 \cos^2 \theta + 30M^5r^2 \cos^2 \theta + 3648r^5 \cos^2 \theta M^2 + 2064r^4 \cos^2 \theta M^3 + 10848r^6 \cos^2 \theta M + 1056M^3r^4 \\
& + 152M^4r^3 - 2848Mr^6 + 2400M^2r^5 + 768r^7 - 30M^5r^2 - M^7 - 12rM^6) r L^4 / [M^2(2r+M)^{14}] \\
& - \frac{4r}{2r+M} \sin^2 \theta L^4 \left[\frac{M(2r-M)}{(2r+M)^2} + r^2 \partial_{rr} + 2 \cot \theta \partial_\theta + \frac{r(6r+M)}{2r+M} \partial_r + \partial_{\theta\theta} \right] F(r, \theta), \tag{C9}
\end{aligned}$$

and the nonzero components of the electric part of the Weyl tensor are given by

$$\begin{aligned}
E_{rr} = & -\frac{8M}{r(2r+M)^2} \\
& + \frac{32}{5} \frac{144r^4 \cos^2 \theta + 36r^2 M^2 \cos^2 \theta - 48r^4 - 32M^2 r^2 + 80Mr^3 - 8M^3 r - M^4}{Mr(2r+M)^8} L^2 \\
& + \frac{64}{25} (704Mr^6 - 7824M^2 r^5 - 3120M^3 r^4 - 400M^4 r^3 - 36M^5 r^2 - 12rM^6 - M^7 + 960r^7 \\
& + 9792r^7 \cos^4 \theta - 6912r^7 \cos^2 \theta - 8256r^6 \cos^2 \theta M + 16128Mr^6 \cos^4 \theta \\
& + 2448M^2 r^5 \cos^4 \theta + 36M^5 r^2 \cos^2 \theta + 960M^4 r^3 \cos^2 \theta + 12864r^5 \cos^2 \theta M^2 \\
& + 6240r^4 \cos^2 \theta M^3) L^4 / [M^2 r(2r+M)^{14}] \\
& + \frac{4}{3} \frac{L^4}{2r+M} \left[\frac{6M(2r-M)}{r(2r+M)^2} - 2r \partial_{rr} + \frac{1}{r} \partial_{\theta\theta} + 2 \frac{2r-5M}{2r+M} \partial_r + \frac{\cot \theta}{r} \partial_\theta \right] F(r, \theta) \tag{C10}
\end{aligned}$$

$$\begin{aligned}
E_{r\theta} = & \frac{768}{5} \sin \theta \cos \theta \frac{r^2(2r-M)}{(2r+M)^7 M} L^2 \\
& + \frac{1536}{25} \sin \theta \cos \theta r^2 (156r^4 \cos^2 \theta - 52r^4 - 78r^3 M \cos^2 \theta \\
& + 186Mr^3 + 26M^2 r^2 - 3M^3 r - M^4) L^4 / [(2r+M)^{13} M^2] \\
& + 4 \frac{L^4}{2r+M} \left(2 \frac{r-M}{2r+M} \partial_\theta - r \partial_{r\theta} \right) F(r, \theta) \tag{C11}
\end{aligned}$$

$$\begin{aligned}
E_{\theta\theta} = & \frac{4Mr}{(2r+M)^2} \\
& - \frac{16}{5} \frac{(168r^4 \cos^2 \theta - 72r^4 - 304Mr^3 + 384r^3 M \cos^2 \theta + 42r^2 M^2 \cos^2 \theta - 38M^2 r^2 - 8M^3 r - M^4)r}{M(2r+M)^8} L^2 \\
& - \frac{32}{25} (23456Mr^6 - 66048M^2 r^5 - 26496M^3 r^4 - 3352M^4 r^3 - 42M^5 r^2 - 12rM^6 - M^7 \\
& + 1152r^7 + 13824r^7 \cos^4 \theta - 11136r^7 \cos^2 \theta + 29616r^4 \cos^2 \theta M^3 \\
& + 89280Mr^6 \cos^4 \theta + 3456M^2 r^5 \cos^4 \theta + 42M^5 r^2 \cos^2 \theta \\
& - 104160r^6 \cos^2 \theta M + 3912M^4 r^3 \cos^2 \theta + 70080r^5 \cos^2 \theta M^2)r L^4 / [M^2(2r+M)^{14}] \\
& + \frac{4}{3} \frac{r}{2r+M} L^4 \left[\cot \theta \partial_\theta - \frac{r(2r-5M)}{2r+M} \partial_r - 2 \partial_{\theta\theta} + r^2 \partial_{rr} - 3 \frac{M(2r-M)}{(2r+M)^2} \right] F(r, \theta) \tag{C12}
\end{aligned}$$

$$\begin{aligned}
E_{\phi\phi} = & \frac{4Mr}{(2r+M)^2} \sin^2 \theta \\
& - \frac{16}{5} \sin^2 \theta r (-384r^3 M \cos^2 \theta + 30r^2 M^2 \cos^2 \theta \\
& + 120r^4 \cos^2 \theta - 26M^2 r^2 - 24r^4 - 8M^3 r + 464Mr^3 - M^4) L^2 / [M(2r+M)^8] \\
& - \frac{32}{25} \sin^2 \theta r (-57024Mr^6 \cos^4 \theta + 5760r^7 \cos^4 \theta + 1440M^2 r^5 \cos^4 \theta \\
& - 2688r^7 \cos^2 \theta - 17136r^4 \cos^2 \theta M^3 - 44352r^5 \cos^2 \theta M^2 + 30M^5 r^2 \cos^2 \theta \\
& - 1992M^4 r^3 \cos^2 \theta + 87648r^6 \cos^2 \theta M + 20256M^3 r^4 - 22048Mr^6 + 768r^7 \\
& - 30M^5 r^2 - M^7 + 2552M^4 r^3 + 50400M^2 r^5 - 12rM^6) L^4 / [M^2(2r+M)^{14}] \\
& - \frac{4}{3} \frac{r}{2r+M} \sin^2 \theta L^4 \left[\frac{3M(2r-M)}{(2r+M)^2} - r^2 \partial_{rr} - \partial_{\theta\theta} + \frac{r(2r-5M)}{2r+M} \partial_r + 2 \cot \theta \partial_\theta \right] F(r, \theta). \tag{C13}
\end{aligned}$$

Next, we find the tensor C_{ab} to $O(L^4)$, from which we construct the Weyl tensor invariants I and J . To $O(L^4)$, we have

$$\begin{aligned}
I = & \frac{12288 M^2 r^6}{(2r+M)^{12}} + 294912 i \frac{\cos \theta M r^7}{(2r+M)^{14}} L \\
& - \frac{294912}{5} \frac{(128 r^4 \cos^2 \theta + 24 r^4 + 144 r^3 M \cos^2 \theta - 8 M r^3 + 32 r^2 M^2 \cos^2 \theta - 14 M^2 r^2 - 8 M^3 r - M^4) r^6}{(2r+M)^{18}} L^2 \\
& - \frac{1179648}{5} i \cos \theta (80 r^4 \cos^2 \theta - 128 r^3 M \cos^2 \theta + 20 r^2 M^2 \cos^2 \theta + 16 r^4 + 112 M r^3 - 136 M^2 r^2 - 7 M^4 \\
& - 56 M^3 r) r^7 L^3 \Big/ [(2r+M)^{20} M] \\
& + \frac{196608}{25} (300 M^7 r + 19 M^8 - 32288 M^2 r^6 + 29712 M^3 r^5 + 21312 M r^7 + 12972 M^4 r^4 \\
& + 1548 M^6 r^2 + 4672 M^5 r^3 + 2496 r^8 - 1920 r^8 \cos^2 \theta + 8640 r^8 \cos^4 \theta \\
& + 43776 r^7 M \cos^2 \theta - 98328 r^4 M^4 \cos^2 \theta - 158016 r^7 M \cos^4 \theta \\
& - 39504 r^5 M^3 \cos^4 \theta - 1356 r^2 M^6 \cos^2 \theta + 540 r^4 M^4 \cos^4 \theta \\
& - 196608 r^5 M^3 \cos^2 \theta - 33408 r^6 M^2 \cos^2 \theta - 233184 r^6 M^2 \cos^4 \theta \\
& - 19056 r^3 M^5 \cos^2 \theta) r^6 L^4 \Big/ [(2r+M)^{24} M^2] \\
& - 4096 \frac{M r^6}{(2r+M)^{11}} L^4 \left[\cot \theta \partial_\theta + 2 \frac{r(2r-5M)}{2r+M} \partial_r + \partial_{\theta\theta} - 2 r^2 \partial_{rr} + 6 \frac{M(10r-M)}{(2r+M)^2} \right] F(r, \theta) \tag{C14}
\end{aligned}$$

and

$$\begin{aligned}
J = & \frac{262144 M^3 r^9}{(2r+M)^{18}} + 9437184 i \cos \theta \frac{M^2 r^{10}}{(2r+M)^{20}} L \\
& - \frac{9437184}{5} \frac{(248 r^4 \cos^2 \theta + 24 r^4 + 264 r^3 M \cos^2 \theta - 8 M r^3 + 62 r^2 M^2 \cos^2 \theta - 14 M^2 r^2 - 8 M^3 r - M^4) M r^9}{(2r+M)^{24}} L^2 \\
& - \frac{75497472}{5} i \cos \theta (172 r^4 \cos^2 \theta + 43 r^2 M^2 \cos^2 \theta + 92 r^3 M \cos^2 \theta - 40 M^3 r + 44 r^4 + 44 M r^3 - 5 M^4 \\
& - 89 M^2 r^2) r^{10} L^3 \Big/ (2r+M)^{26} \\
& + \frac{25165824}{25} (111 M^7 r + 7 M^8 - 74096 M^2 r^6 + 13116 M^3 r^5 + 28656 M r^7 + 3720 M^4 r^4 \\
& + 594 M^6 r^2 + 1708 M^5 r^3 + 10752 r^8 \cos^2 \theta - 31728 r^7 M \cos^4 \theta \\
& - 153264 r^6 M^2 \cos^4 \theta - 7932 r^5 M^3 \cos^4 \theta + 1800 r^4 M^4 \cos^4 \theta \\
& - 12504 r^3 M^5 \cos^2 \theta - 978 r^2 M^6 \cos^2 \theta - 60240 r^4 M^4 \cos^2 \theta \\
& + 10944 r^7 M \cos^2 \theta + 129312 r^6 M^2 \cos^2 \theta - 122160 r^5 M^3 \cos^2 \theta - 384 r^8 \\
& + 28800 r^8 \cos^4 \theta) r^9 L^4 \Big/ [(2r+M)^{30} M] \\
& - 131072 \frac{M^2 r^9}{(2r+M)^{17}} L^4 \left[\cot \theta \partial_\theta + 2 \frac{r(2r-5M)}{2r+M} \partial_r + \partial_{\theta\theta} - 2 r^2 \partial_{rr} + 6 \frac{M(10r-M)}{(2r+M)^2} \right] F(r, \theta). \tag{C15}
\end{aligned}$$

APPENDIX D: THE BOWEN–YORK BB RADIATION SCALAR IS INDEPENDENT OF $F(r, \theta)$

In this Appendix we outline a calculation that shows why the speciality index S , and hence the BB radiation scalar ξ^0 , is independent of the $O(L^4)$ terms in the conformal factor.

Let us expand the curvature invariants I and J to $O(L^4)$ as

$$I = \sum_{k=0}^4 i_k L^k \quad , \quad J = \sum_{k=0}^4 j_k L^k \tag{D1}$$

where the expansion coefficients i_k and j_k are given by (C14) and (C15). The only coefficients that depend on $F(r, \theta)$

are i_4 and j_4 . The speciality index S is given by (11) and can also be expanded in powers of L up to order $O(L^4)$ as

$$S = \sum_{k=0}^4 s_k L^k. \quad (\text{D2})$$

The expansion coefficients can be found from the definition of S and the expansion coefficients for I and J .

The leading order term in S is unity. A straightforward calculation shows that the next contributing order is at $O(L^4)$. What remains to be shown is that the $O(L^4)$ term $s_4 L^4$ is independent of $F(r, \theta)$. It turns out that the only dependence of s_4 on either i_4 or j_4 is through the combination $2i_0 j_4 - 3j_0 i_4$. A direct substitution finds that this combination equals exactly zero, which completes the proof.

The BB scalar ξ^0 is proportional to I times a power series in $S - 1$, the leading order term being of $O(S - 1)$. Consequently, the earliest order at which $F(r, \theta)$ can contribute is at $O(L^8)$. Specifically, it does not contribute at $O(L^4)$, which is the leading order for the BB scalar.

- [1] T.W. Baumgarte and S.L. Shapiro, Phys. Rept. **376**, 41 (2003).
- [2] M. Shibata, K. Taniguchi and K. Uryū, Phys. Rev. D **68**, 084020 (2003).
- [3] P. Marronetti, M.D. Duez, S.L. Shapiro and T.W. Baumgarte, Phys. Rev. Lett. **92**, 141101 (2004)
- [4] B. Brügmann, W. Tichy and N. Jansen, Phys. Rev. Lett. **92**, 211101 (2004).
- [5] F. Pretorius, submitted (also gr-qc/0507014)
- [6] G.B. Cook, Living Rev. Rel. **5**, 1 (2000).
- [7] H.P. Pfeiffer, G.B. Cook and S.A. Teukolsky, Phys. Rev. D **66** 024047 (2002).
- [8] C. Beetle and L.M. Burko, Phys. Rev. Lett. **89**, 271101 (2002).
- [9] C. Beetle, M. Bruni, L.M. Burko and A. Nerozzi, Phys. Rev. D **72**, 024013 (2005).
- [10] A. Nerozzi, C. Beetle, M. Bruni, L.M. Burko, and D. Pollney, Phys. Rev. D **72**, 024014 (2005).
- [11] P. Szekeres, J. Math. Phys. **6**, 1387 (1965).
- [12] R.M. Wald, *General Relativity* (U. of Chicago Press, Chicago, 1984), Eq. (7.2.40); S.M. Carroll, *Spacetime and Geometry* (Addison Wesley, San Francisco, 2004), Eq. (D.41).
- [13] J. Baker and M. Campanelli, Phys. Rev. D **62** 127501 (2000).
- [14] J. Weber and J.A. Wheeler, Rev. Mod. Phys. **29**, 509 (1957).
- [15] S.A. Teukolsky, Phys. Rev. D **26**, 745 (1982).
- [16] J.M. Bowen and J.W. York, Jr., Phys. Rev. D **21**, 2047 (1980).
- [17] A. Garat and R.H. Price, Phys. Rev. D **61** 124011 (2000).
- [18] R.J. Gleiser, C.O. Nicasio, R.H. Price and J. Pullin, Phys. Rev. D **57**, 3401 (1998).
- [19] H.P. Pfeiffer, in Proceedings of the Miami Waves Conference (2004), in press [gr-qc/0412002].
- [20] C. Cherubini, D. Bini, M. Bruni, and Z. Perjes, Class. Quantum Grav. **21**, 4833 (2004).
- [21] E. Berti, F. White, A. Maniopolou, and M. Bruni, Mon. Not. Roy. Astron. Soc. **358**, 923 (2005).